Title	Convective and periodic motion driven by a chemical wave
Author(s)	Kitahata, H; Aihara, R; Magome, N; Yoshikawa, K
Citation	JOURNAL OF CHEMICAL PHYSICS (2002), 116(13): 5666-5672
Issue Date	2002-04-01
URL	http://hdl.handle.net/2433/49852
Right	Copyright 2002 American Institute of Physics. This article may be downloaded for personal use only. Any other use requires prior permission of the author and the American Institute of Physics.
Type	Journal Article
Textversion	publisher

Convective and periodic motion driven by a chemical wave

Hiroyuki Kitahata, Ryoichi Aihara,[a] Nobuyuki Magome, and Kenichi Yoshikawa[b]
Department of Physics, Graduate School of Science, Kyoto University and CREST, Kyoto 606-8502, Japan

(Received 3 December 2001; accepted 9 January 2002)

The generation of convective flow by a chemical wave was studied experimentally on a mm-sized droplet of Belousov–Zhabotinsky (BZ) reaction medium. A propagating chemical wave causes a transient increase in interfacial tension, and this local change in interfacial tension induces convection. The observed flow profile was reproduced with a numerical simulation by introducing the transient increase in interfacial tension to a modified Navier–Stokes equation coupled with a chemical kinetic equation; a modified Oregonator. We also observed the periodic motion of a BZ droplet floating on an oil phase. Such periodic motion is attributed to the rhythmic change in interfacial tension. The observed periodic convective motion coupled with a chemical reaction is discussed in relation to chemo-mechanical energy transduction under isothermal conditions. © *2002 American Institute of Physics.* [DOI: 10.1063/1.1456023]

I. INTRODUCTION

In living organisms, vectorial work is generated through the dissipation of chemical energy under isothermal conditions.[1,2] For example, muscles macroscopically extend and contract using the chemical energy of adenosine triphosphate (ATP), and motor proteins, actins and miosins, play an essential role in producing vectorial work.[3] In cellular motion, kinesin molecules exhibit rhythmic conformational changes in cooperation with dynin molecules, accompanied by the dissipation of ATP.[4] In general, chemical reactions such as the hydrolysis of ATP, are described by a mass-action law, i.e., the kinetics is represented as a function of scalar variables. According to the Curie–Prigogine principle, coupling between scalar and vectorial variables is prohibited under isotropic conditions within the framework of linear nonequilibrium theory.[5,6] The intrinsic mechanism of energy transduction from scalar chemical energy into vectorial mechanical work has been a longstanding problem in natural science and technology. Over the past decade, there has been a considerable controversy regarding the generation of vectorial motion with a ratchet-type periodic potential under thermal fluctuation.[7–9] Most of these studies have discussed the directed motion of an object accompanied by a periodic change between ratchet-type and flat potentials. In such models, it has been assumed that the potential itself exhibits no fluctuation except for during the sudden change between the two extremes, i.e., the spatial correlation of noise has been almost completely ignored. However, since actual motor proteins are typically on the order of several nm in size, the molecular motor itself should exhibit significant conformational fluctuations, coupled with the thermal noise in the environment. With regard to the mechanism of a nm-sized machine, it may be useful to address the serious problem regarding adiabatic conditions in the Carnot cycle and a similar problem in the ratchet model, i.e., the static potential between the sudden changes. In general, the characteristic time for thermal diffusion scales as

$$\Delta t \approx \frac{(\Delta x)^2}{D_T}, \tag{1}$$

where D_T is the thermal diffusion constant of the system and Δx is the characteristic length. Since the thermal diffusion constant of water is about 1×10^{-7} m^2 s^{-1}, Δt becomes 1×10^{-11} s (10 ps) at the length scale of $\Delta x = 1$ nm. Since the conformational transition of working proteins with the size of several nm is characteristically longer than ms, the thermal energy produced by a chemical reaction dissipates much faster than the characteristic time of the conformational transition. Thus, the energy derived from the chemical energy is distributed to the huge degrees of motional freedom in the system, according to the equipartition theorem, within a time scale of less than ms. Thus, in general, it is difficult to realize an adiabatic process in nm-sized systems.

In the present study, we tried to develop a system in which chemical energy is converted into mechanical work. We adopted the Belousov–Zhabotinsky (BZ) reaction, a well-known oscillatory chemical reaction. Under well-stirred conditions, BZ medium shows a rhythmic change between oxidized and reduced states. When the medium is allowed to stand without stirring, chemical waves are generated spontaneously, forming target or spiral patterns.[10] Such chemical waves have been analyzed under the framework of reaction-diffusion equations, i.e., no convection is considered. In fact, most of the experimental studies on the spatio-temporal structure of BZ medium have reported seemingly negligible effects of convection coupled with the chemical reaction. Only a few reports have described the appearance of convective flow.[11–21] Unfortunately, the reproducibility of convective motion in previous studies does not seem to have been satisfactory, and sometimes the induced motion did not directly correspond to the rhythmic behavior of the reaction in

[a]Present address: Frontier Research System, RIKEN, Wako, Saitama 351-0198, Japan.
[b]Author to whom correspondence should be addressed. Telephone: +81-75-753-3812; Fax: +81-75-753-3779; electronic mail: yoshikaw@scphys.kyoto-u.ac.jp

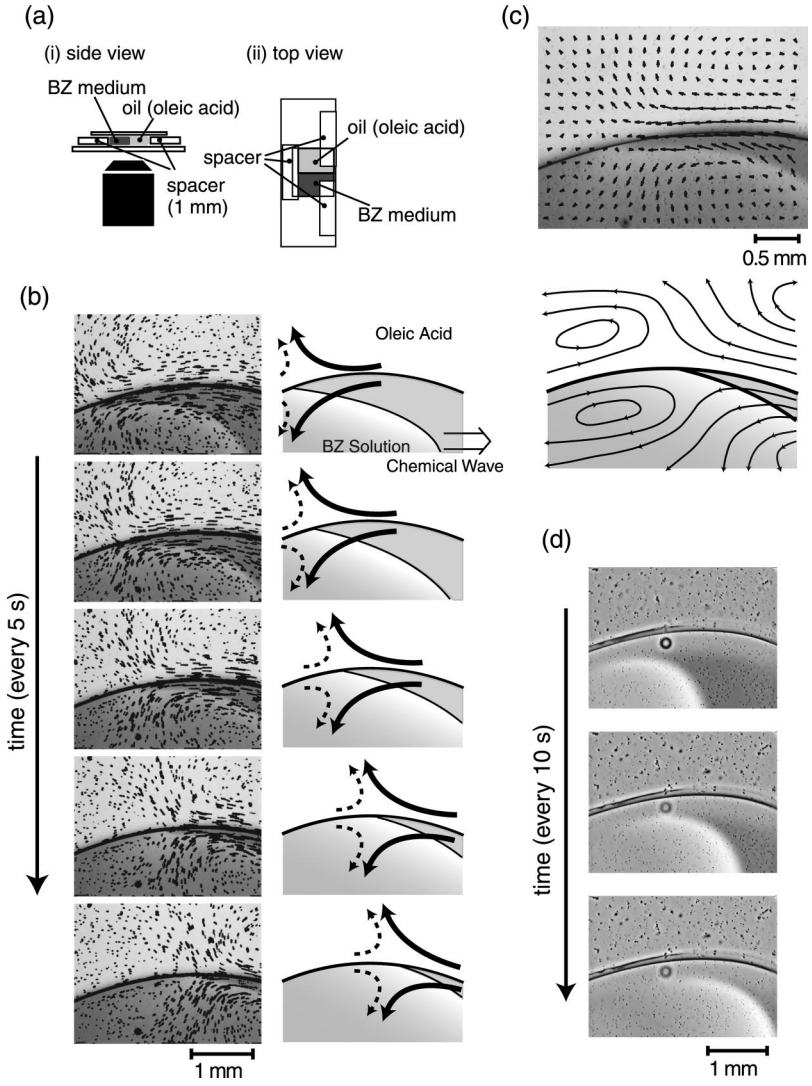

FIG. 1. (a) Schematic representation of the experimental apparatus. (i) Side view and (ii) top view are shown. (b) Results of convective flow on the horizontal plane. The profiles of fluid lines in 1 s are shown at the intervals of 5 s. The upper phase is oleic acid and the lower phase is the BZ medium; the chemical wave propagates from left to right. Convective flow is generated towards the wave front on both sides. (Left column) Schematic illustrations are also given to show the direction of convective flow (right column). (c) Profile of fluid velocity calculated with flow analysis software. The chemical wave propagates from left to right. (d) Disappearance of convective flow due to an inhibitor, iodine, of the chemical reaction. Pure oleic acid was replaced by oleic acid with iodine. The chemical wave propagates from left to right in the bulk solution, but does not reach the interface, and no convective flow is induced.

a satisfactory manner. Theoretical analyses regarding the observed convective motion have not reproduced the complete profiles of the convection induced by the chemical reaction. On the other hand, the generation of a rhythmic change in interfacial tension on the order of several $\mathrm{mN\,m^{-1}}$, driven by the rhythmic change in the BZ reaction has recently been reported.[22] This periodic change in interfacial tension has been attributed to the change in the surface activity of the iron-catalyst between $[\mathrm{Fe(phen)_3}]^{2+}$ and $[\mathrm{Fe(phen)_3}]^{3+}$. Thus, it is expected that the convective motion driven by interfacial tension should be enhanced in a smaller system, due to the increase in the ratio of surface A to volume V, A/V.[23] In this study, using a small droplet of BZ medium, the effect of breaking the symmetry of isotropy becomes dominant and induces a directional convective motion in the chemical droplet.

II. EXPERIMENTAL RESULTS

A. Convective flow induced by chemical waves

All chemicals were analytical grade reagents and used without further purification. An aqueous solution of ferroin, tris (1,10-phenanthroline) iron (II) sulfate, was prepared by mixing stoichiometric amounts of 1,10-phenanthroline and ferrous sulfate in pure water. The water was purified with a Millipore-Q system. BZ medium, in the excitable state, contains 0.15 M sodium bromate ($\mathrm{NaBrO_3}$), 0.30 M sulfuric acid ($\mathrm{H_2SO_4}$), 0.10 M malonic acid ($\mathrm{CH_2(COOH)_2}$), 0.03 M potassium bromide (KBr), and 5.0 mM ferroin ($[\mathrm{Fe(phen)_3}]^{2+}$). To visualize the convective flow, polystyrene beads (General Science Corporation, 10 μm diam) were dispersed throughout the medium. BZ medium and oleic acid were situated between two glass plates (clearance, 1.0 mm). A chemical wave was initiated using silver wire. The region near the interface between BZ medium and oleic acid was observed from below by an inverted microscope (Nikon DIAPHOT-TMD), as schematically shown in Fig. 1(a).

Figure 1(b) shows the convective flow that accompanied the propagation of a chemical wave in the BZ medium, where the flow of the tracer beads ($\phi = 10\ \mu$m) was visualized as the accumulation of video frames over 1.0 s, together with image-processing to compensate for the nonuniformity of the illumination.[24] Using the extended constraint equation with spatio-temporal local optimization[25] and motion stabilization using a reliability process, the flow profiles were calculated more schematically, as shown in Fig. 1(c). On the

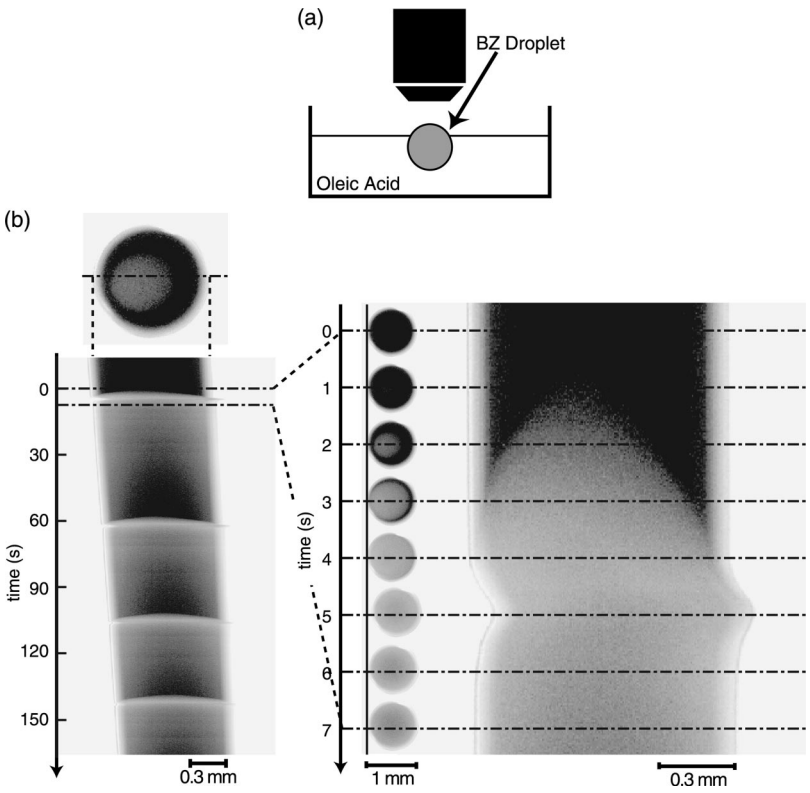

FIG. 2. (a) Schematic representation of the experimental apparatus. The volume of the droplet is 1 μl, and thus the diameter is $\approx$1 mm. (b) Left-hand side: spatio-temporal plot for the intersection on a BZ droplet as shown on the above. Right-hand side: magnification of the time-scale on the spatio-temporal plot. The bright and dark regions correspond to the oxidized and reduced states, respectively.

front of the chemical wave, large convective flow, parallel to the interface and opposite the direction of movement of the chemical wave, is induced in both the water and oil phases. Parallel flow in the same direction as the chemical wave is observed on the back of the chemical wave at the interface. In both the water and oil phases near the intersection of the chemical wave with the interface, the flow sinks into the bulk phases. Figure 1(d) shows the results of an experiment in which iodine was added to the oil phase. In this experiment, no convective flow was generated, despite the appearance of a chemical wave. Iodine is a potent inhibitor of the BZ reaction.[26,27] The iodine in the oil phase is expected to inhibit wave generation near the interface, due to its diffusion from the oil to the aqueous phase through the interface. Thus, the absence of convective flow can be attributed to the failure of the chemical wave to propagate to the interface. This convective flow is clearly caused by the difference in interfacial tension between the oxidized and the reduced states.[22]

B. Spontaneous motion of a droplet of BZ medium

Using the experimental system in Fig. 2(a), we observed the motion of a 1 μl droplet of BZ medium floating on a layer of oleic acid. In this experiment, the concentration of sulfuric acid was 0.60 M, whereas the concentrations of the other chemicals were the same as in Sec. II A, where the medium is in an oscillatory state.

Figure 2(b) reveals the whole motion of a BZ droplet floating on the surface of oleic acid. The spatio-temporal plot (left-handed side) at the broken line indicates a translational motion of the droplet accompanied by the generation of chemical wave. On the right-hand side of Fig. 2(b), the spatio-temporal plot of the BZ droplet with an extension of time-scale is shown to indicate the motion with the propagation of a chemical wave, where the chemical wave propagates toward the right within the droplet. When the chemical wave touches the left interface, the droplet moves toward the right. Then, the droplet moves back to the left, resulting in a small net translational motion to the right.

III. NUMERICAL RESULTS

The Navier–Stokes equation modified with an interfacial tension term is adopted for the numerical calculation. For simplicity, incompressibility ($\nabla \cdot \mathbf{v}=0$) is assumed. The modified Navier–Stokes equation is written as

$$\rho\left(\frac{\partial \mathbf{v}}{\partial \mathbf{t}}+(\mathbf{v}\cdot\nabla)\mathbf{v}\right)=\eta\Delta\mathbf{v}+\mathbf{F}_i, \tag{2}$$

where ρ is the density of the fluid, $\mathbf{v}$ is the fluid velocity, η is viscosity, and $\mathbf{F}_i$ is interfacial tension.

For simplicity, we neglect the change in pressure, due to the rather slow rate of both the chemical wave and the accompanying convective flow. Cartesian coordinates are set so that the interface meets the x axis. For the kinetics of an oscillatory chemical reaction, a two-variable Oregonator is adopted,[28–30]

$$\frac{\partial U}{\partial t}=f(U,V)+D_U\Delta U-\mathbf{v}\cdot\nabla U, \tag{3}$$

$$\frac{\partial V}{\partial t}=g(U,V)+D_V\Delta V-\mathbf{v}\cdot\nabla V, \tag{4}$$

$$f(U,V)=\frac{1}{\varepsilon}\left(U(1-U)-fV\frac{U-q}{U+q}\right), \tag{5}$$

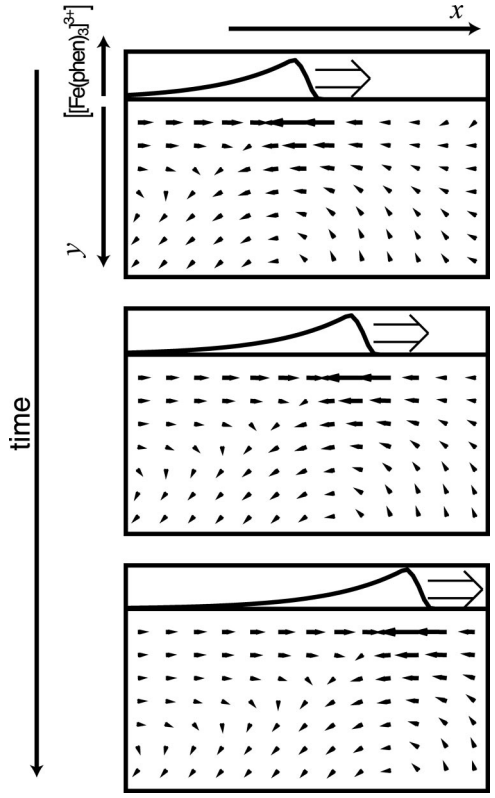

FIG. 3. The results of a numerical calculation using a modified Navier–Stokes equation. The chemical wave propagates and convective flow is generated towards the wave front on both sides. The flow on the front of the chemical wave is stronger than that on the back.

$$g(U,V)=U-V, \tag{6}$$

where U and V are the concentrations of the activator and the inhibitor, respectively; $f(U,V)$ and $g(U,V)$ are the reaction terms; and f, ε, and q are parameters that represent the threshold, excitability, and nondimensional reaction rate constant, respectively. In the Oregonator model, the activator and inhibitor correspond to bromous acid ($HBrO_2$), and oxidized iron-catalyst ($[Fe(phen)_3]^{3+}$, ferriin), respectively. To take into account the flow of the reactants, advection terms ($\mathbf{v}\cdot\nabla U$ and $\mathbf{v}\cdot\nabla V$) are added.

Interfacial tension works only at the interface in the direction parallel to the interfacial plane, and it is assumed that the tension is proportional to the gradient of the concentration of ferriin,[22]

$$\mathbf{F}_i=F_i\mathbf{e}_x\propto\frac{\partial V}{\partial x}\mathbf{e}_x. \tag{7}$$

The advection terms are neglected for simplification. Thus, only the influence of the chemical reaction on convection, but not feedback, is considered. The results of a numerical calculation using Eqs. (2)–(7) by the Euler method are shown in Fig. 3. The chemical wave propagates at a constant velocity, and near the interface flow is induced towards the chemical wave. The flow on the front of the chemical wave is stronger than that on the back, corresponding to the experimental trend.

Using this framework, the profile of interfacial tension can be estimated. The x and y components of fluid velocity $\mathbf{v}$ are supposed to be u and v, respectively. The x component of Eq. (2) is

$$\rho\left(\frac{\partial u}{\partial t}+u\frac{\partial u}{\partial x}+v\frac{\partial u}{\partial y}\right)=\eta\left(\frac{\partial^2 u}{\partial x^2}+\frac{\partial^2 u}{\partial y^2}\right)+F_i. \tag{8}$$

As we approach the region near the interface, the velocity parallel to the interfacial plane, u, is greater than that perpendicular to the plane, v. Thus we can neglect the term $\rho v\,\partial u/\partial y$. The term $\eta\partial^2 u/\partial y^2$ represents diffusion in the y direction. The characteristic time for passing of the chemical wave, Δt, is about 10 s based on the experimental results. Therefore, the characteristic depth of the region, Δy, in which fluid moves attached to the interface is calculated as

$$\Delta y\sim\sqrt{\frac{\eta}{\rho}\Delta t}\cong 0.3\ \text{cm}. \tag{9}$$

From the experiments, the viscosities of the BZ medium and oleic acid were $1.1\times10^{-2}\ \text{g cm}^{-1}\,\text{s}^{-1}$ and $3.5\times10^{-1}\ \text{g cm}^{-1}\,\text{s}^{-1}$, respectively. In this calculation, the viscosity and density of BZ medium are adopted. From now on, only the x component is considered, and the interfacial tension is taken as the force working in the region within Δy from the interface. In this framework, the interfacial tension can be considered a volume force, and can be combined with an interfacial tension constant γ as follows:

$$\frac{\partial\gamma}{\partial x}=F_i\Delta y. \tag{10}$$

Since the chemical wave propagates at a constant velocity, c, the fluid velocity profile, u, satisfies the differential equation,

$$\frac{\partial u}{\partial t}=c\frac{\partial u}{\partial x}. \tag{11}$$

From the experiments, the velocity of the chemical wave parallel to the interface is $c=0.01\ \text{cm s}^{-1}$. Thus, Eq. (8) can be simplified to a one-dimensional ordinary differential equation,

$$\rho\left(c\frac{du}{dx}+u\frac{du}{dx}\right)=\eta\frac{d^2u}{dx^2}+F_i. \tag{12}$$

The fluid velocity profile near the interface was measured, and the results are shown in Fig. 4(a). Using these results, the first-order derivative, the second-order derivative, and the interfacial tension profile are calculated. The profile of the gradient of the interfacial tension, $d\gamma/dx$, is shown in Fig. 4(b). Using this profile, the profile of the interfacial tension, $\Delta\gamma$, is calculated by integration, as shown in Fig. 4(c). The profile of the chemical wave is shown in Fig. 4(d), which is obtained from a quantitative analysis of the color in the reacting solution. It is clear that the profile of the chemical wave corresponds to the profile of the interfacial tension, except for the differences in their maxima and widths. These differences are attributed to the effect of the convective motion of the reacting solution. As in Figs. 4(b) and 4(c), the portion of the fluid in the reduced state (low $[Fe(phen)_3]^{3+}$) is pulled toward the front of the chemical wave. This con-

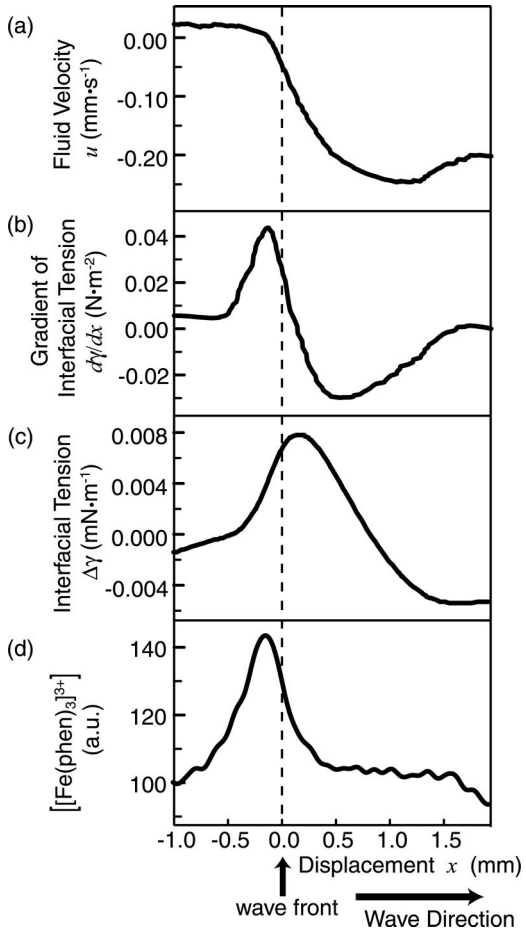

FIG. 4. Spatial profile of various physicochemical variables deduced from the experimental results on convection generated by the BZ reaction, as in Fig. 1. (a) Fluid velocity, u, parallel to the interface in the region near the interface. The chemical wave propagates from left to right, and the origin is set at the position of the wave front. (b) The gradient of interfacial tension, $d\gamma/dx$, calculated from the fluid velocity profile. (c) Interfacial tension, $\Delta\gamma$, calculated by integration of (b). (d) The chemical wave as represented by a change in the concentration of ferriin ($[\mathrm{Fe(phen)_3}]^{3+}$).

vective effect causes retardation of the phase of the oscillatory reaction of the wave front, together with narrowing of the chemical wave. The change in interfacial tension between the oxidized state and the reduced state is on the order of 0.01 mN m^{-1}, as in Fig. 4(c). This is about 1% of the value in a previous report,[22] where the interfacial tension was measured under the condition that the BZ medium was stirred and the medium was uniform. In the present experiment, we estimated the change in interfacial tension under the condition of propagation of a chemical wave without stirring the reaction medium. Since the interfacial tension on the front of the wave is opposite that on the back, the net velocity may be damped. In the analysis adopted above, we assumed that the system was two-dimensional, however, the actual system was the space between two glass plates. The fluid must be effected by the friction from the glass plates, which should disturb the motion of the fluid. In addition, there would be a rather large damping effect, i.e., flow in the aqueous phase inevitably induces flow in the oil phase, as discussed later. The discrepancy in the amplitude of the change in interfacial tension can be attributed to these effects. This estimation of the interfacial tension profile from the fluid velocity profile might be useful in an analysis of fluid dynamics.

IV. DISCUSSION

Since Miike *et al.* reported the convective flow induced by chemical waves of the BZ reaction in a system with a free surface,[11–13] there are several reports of both experimental results and theoretical analyses on this subject.[14–21] Some have insisted that the convection is induced by gravitational instability due to density inversion generated by the reaction.[14,17] In the present study, we performed the observation on the interfacial plane parallel to the horizontal plane to eliminate the effects of gravitation. As Fig. 1(b) clearly shows, convective flow appears in the absence of a gravitational effect. Matthiessen *et al.* stressed the importance of the effect of a spatial gradient in the interfacial tension, regarding the mechanism of spontaneous convection in BZ medium. Unfortunately, they discussed their results based on a numerical study of time-independent profiles of interfacial tension.[18] To achieve a better understanding of the mechanism of convection coupled with reaction-diffusion, a model calculation of a system with a traveling wave, or a time-dependent change in interfacial tension, is necessary. Our model explicitly includes time. The results of this numerical calculation prove that the difference in interfacial tension generates convective flow. This convective motion can be regarded as the result of chemomechanical energy transduction using the BZ reaction. However, the BZ droplet is a better system in which chemical energy is converted into mechanical work under isothermal conditions.

Hence, we can discuss the mechanism of this motion of the BZ droplet. The modified Navier–Stokes equation [Eq. (2)] and the equation of interfacial tension [Eq. (7)] are available. The Reynolds number is calculated to be

$$R=\frac{\rho u l}{\eta}=\frac{1\ \ \mathrm{g\,cm^{-3}}\cdot 0.01\ \ \mathrm{cm\,s^{-1}}\cdot 0.1\ \ \mathrm{cm}}{0.01\ \ \mathrm{g\,cm^{-1}\ s^{-1}}}=0.1,$$

where l is the characteristic length of the system, or the diameter of the droplet, and u is the characteristic velocity of the fluid. This value is small enough for the nonlinear term to be neglected.[31] Equation (7) is simplified as follows:

$$\rho\frac{\partial \mathbf{v}}{\partial t}=\eta\Delta\mathbf{v}+\mathbf{F}_i. \tag{13}$$

Now, considering just the local area shown in Fig. 5(a), it is clear that, near the interface, convective flow is generated from the reduced-state region (less interfacial tension) to the oxidized-state region (more interfacial tension). We can ask what will happen when this convective flow is generated at the interface between two liquids with different viscosities. Considering only the direction perpendicular to the interfacial plane, Eq. (13) becomes a one-dimensional parabolic partial differential equation,

$$\rho\frac{\partial u}{\partial t}=\frac{\partial^2 u}{\partial y^2}+F_i. \tag{14}$$

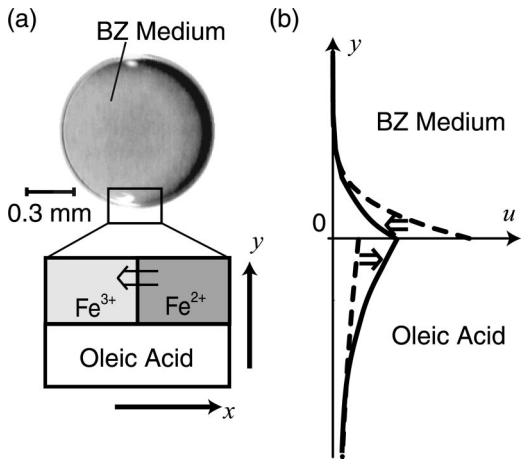

FIG. 5. Effect of a temporal change in interfacial tension with a chemical wave in a two-phase system of aqueous BZ medium and oleic acid. (a) Top view of the droplet of BZ medium generating a chemical wave. (b) Solid line, velocity profile with drag between the interfacial layers; broken line, velocity profile in the absence of drag.

It is assumed that the constant interfacial tension operates during some period,

$$F_i = \begin{cases} u_0 \delta(y) & (0 < t < t_0) \\ 0 & (\text{otherwise}). \end{cases} \tag{15}$$

Equations (14) and (15) can be solved using the Green function method by analogy with a diffusion equation (see Appendix). The solution of Eqs. (14) and (15) is

$$u(t_0, y) = u_0 \left\{ \sqrt{\frac{\rho t_0}{\pi \eta}} \exp\left(-\frac{\rho y^2}{4 \eta t_0} \right) - \frac{y\rho}{2\eta} \left(1 - \mathrm{erf}\left(\sqrt{\frac{\rho}{4 \eta t_0}} y \right) \right) \right\}, \tag{16}$$

where erf(x) is the error function defined as

$$\mathrm{erf}(x) = \frac{1}{\sqrt{\pi}} \int_{-\infty}^{x} \exp(-y^2) dy. \tag{17}$$

From Eq. (16), if each phase existed independently, the fluid velocity at the interface would be

$$u(t_0, 0) = u_0 \sqrt{\frac{\rho t_0}{\pi \eta}}. \tag{18}$$

Without any friction at the interface, the fluid velocity at the interface in oleic acid would be about six times that in BZ medium due to the difference in viscosity between the two phases. In the real system, however, the friction exists between two fluids with different velocities. Thus, momentum should be exchanged between the oleic acid phase and the BZ medium phase [see Fig. 5(b)]. As a result, the BZ medium phase receives momentum, or force, in the opposite direction to the flow, which brings about motion of the droplet. The process by which the BZ droplet returns has not yet been explained, but may be related to the viscoelasticity of oleic acid.

The Curie–Prigogine principle insists that scalar and vectorial variables cannot couple with each other under isotropic conditions within the framework of linear nonequilibrium theory. The BZ reaction cannot be described with linear equations, due to the autocatalytic process in the chemical reaction. In addition, this nonlinearity causes a chemical wave, which breaks the symmetry of isotropy. As the system becomes smaller, the effect of the boundary should become more prominent.

The motive force of the droplet is the gradient of interfacial tension, which is proportional to the length of where the chemical wave touches the interface between the BZ medium and oleic acid. Hence, the interfacial tension is proportional to r, the system size,

$$|\mathbf{F}_i| \propto \gamma r. \tag{19}$$

On the other hand, the mass is proportional to the cube of the system size,

$$M = \rho r^3. \tag{20}$$

Hence, the acceleration α is proportional to r^{-2},

$$|\mathbf{F}_i| = M\alpha, \tag{21}$$

$$\alpha \propto \frac{\gamma}{\rho} \frac{1}{r^2}. \tag{22}$$

The BZ droplet moves more as the size of the system gets smaller. However, the chemical reaction is hard to activate, when the system is very small. Moreover, the time lag from when the chemical wave touches one side to when it touches the other side becomes shorter, so the droplet moves less. Considering these factors, a system size of 1 mm is suitable for observing direct coupling between a chemical reaction and convection.

Generally, a system should follow a cyclic pathway in phase space as it produces mechanical work. Integration of the area surrounded by the pathway corresponds to the mechanical work the system produces in one cycle. Projected onto one-variable space, the phase point oscillates as the system follows the cyclic pathway. In fact, by single-molecular observation, it has been confirmed that a kinesin molecule exhibits a rhythmic conformational change.[4] Macroscopic thermal engines and microscopic molecular motors are the same in this aspect, but they have quite different features from each other. Artificial thermal engines take advantage of heat flow due to a temperature gradient. This mechanism is available only when the system is big enough to be able to maintain its temperature against thermal diffusion. Thus, adiabatic conditions can only exist in a system larger than a certain size. With the second law of thermodynamics, thermal efficiency is maximum when every process in the cycle is quasi-static, and the maximum efficiency is $1 - T_C/T_H$, where T_C and T_H are the temperature of the colder and hotter heat baths, respectively. Hence, a thermal engine cannot work in an isothermal system. Moreover, since thermal fluctuation is proportional to the root of the system size, such fluctuation is enhanced as the system size becomes smaller. When this fluctuation exceeds the typical size of the system, the system cannot work as a thermal engine. Based on experiments, it has been shown that molecular motors are typically on the order of several nm in size, and that the typical

order of the force is several pN. Thus, the typical order of the mechanical work produced by molecular motors is about 10^{-21} J. On the other hand, the typical order of thermal fluctuation is $k_BT \sim 4\times10^{-21}$ J at about room temperature. Therefore, it is clear that molecular motors operate under quite a different mechanism than artificial thermal engines. Molecular motors may operate through a mechanism that includes the bifurcation induced by nonlinear and nonequilibrium conditions. This enables the system to follow a cyclic pathway, or a limit cycle, spontaneously. The system can produce mechanical work against thermal fluctuation. However, nonlinear and nonequilibrium conditions are not sufficient to produce mechanical work in an effective manner. Breaking the symmetry of isotropy, spontaneously or not, is essential to produce vectorial work from scalar chemical energy. In the present case, by using a small droplet, a time-lag is made for the chemical wave touching the interface. This time-lag breaks the isotropy and vectorial work is, thus, produced from scalar chemical energy.

V. CONCLUSION

Convective flow was induced by a change in interfacial tension between the oxidized state and the reduced state in the BZ reaction. Thus, the directed motion was generated by chemical waves, as a kind of chemical engine working under isothermal conditions. Since chemical reactions can generally be described by nonlinear kinetic equations with several variables, i.e., concentrations of the chemical species, further studies on chemomechanical energy transduction accompanied by a nonlinear chemical wave should be promising.

ACKNOWLEDGMENTS

The authors would like to thank T. Ichino for his helpful discussion and assistance, and Professor H. Miike and Dr. A. Osa for their kind advice with the technique for image processing. This work was supported in part by a Grant-in-Aid from the Ministry of Education, Science, Sports, and Culture of Japan.

APPENDIX: CALCULATION

Equations (14) and (15) are one-dimensional diffusion equations with constant inflow at the origin. The Green function for the one-dimensional diffusion, $G(y)$, is

$$\frac{\partial G}{\partial t} = D\frac{\partial^2 G}{\partial y^2} \quad \text{with} \quad G(t=0,y)=\delta(y), \tag{A1}$$

$$G(t,y) = \frac{1}{\sqrt{4\pi Dt}}\exp\left(-\frac{y^2}{4Dt}\right). \tag{A2}$$

When a constant inflow, u_0, exists at the origin from $t=0$ to $t=t_0$, the distribution can be written explicitly using the Green function,

$$u(t_0,y) = u_0\int_0^{t_0} G(t,y)dt. \tag{A3}$$

Equation (A3) can be calculated analytically, and the solution is

$$u(t_0,y) = u_0\left\{\sqrt{\frac{t_0}{\pi D}}\exp\left(-\frac{y^2}{4Dt_0}\right) - \frac{y}{2D}\left(1-\mathrm{erf}\left(\frac{y}{\sqrt{4Dt_0}}\right)\right)\right\}. \tag{A4}$$

This result is used in Eq. (16), where the diffusion coefficient D corresponds to η/ρ.

[1] E. Schrödinger, *What is Life?* (Cambridge University Press, Cambridge, 1944).
[2] K. Yoshikawa and H. Noguchi, Chem. Phys. Lett. **133**, 10 (1999).
[3] K. Yasuda, Y. Shindo, and S. Ishiwata, Biophys. J. **70**, 1823 (1996).
[4] M. Kikkawa, E. P. Sablin, Y. Okada, R. J. Fletterick, and N. Hirokawa, Nature (London) **411**, 439 (2001).
[5] S. R. de Groot and P. Mazur, *Non-Equilibrium Thermodynamics* (North–Holland, Amsterdam, 1962).
[6] A. Katchalsky and P. F. Curran, *Nonequilibrium Thermodynamics in Biophysics* (Harvard University Press, Cambridge, 1965).
[7] R. P. Feynman, R. B. Leighton, and M. Sands, *The Feynman Lectures on Physics* (Addison–Wesley, Massachusetts, 1963), Vol. I.
[8] J. Rousselet, L. Salome, A. Ajdari, and J. Prost, Nature (London) **370**, 446 (1994).
[9] K. Sekimoto, J. Phys. Soc. Jpn. **66**, 1234 (1997).
[10] R. Kapral and K. Showalter, *Chemical Waves and Patterns* (Kluwer Academic, Dordrecht, 1995).
[11] H. Miike, S. C. Müller, and B. Hess, Chem. Phys. Lett. **144**, 515 (1988).
[12] H. Miike, S. C. Müller, and B. Hess, Phys. Rev. Lett. **61**, 2109 (1988).
[13] H. Miike, S. C. Müller, and B. Hess, Phys. Lett. A **141**, 25 (1989).
[14] J. A. Pojman and I. R. Epstein, J. Phys. Chem. **94**, 4966 (1990).
[15] H. Miike and S. C. Müller, Chaos **3**, 21 (1993).
[16] K. Matthiessen and S. C. Müller, Phys. Rev. E **52**, 492 (1995).
[17] H. Wilke, Physica D **86**, 508 (1995).
[18] K. Matthiessen, H. Wilke, and S. C. Müller, Phys. Rev. E **53**, 6056 (1996).
[19] T. Sakurai, H. Miike, E. Yokoyama, and S. C. Müller, J. Phys. Soc. Jpn. **66**, 518 (1997).
[20] T. Sakurai, E. Yokoyama, and H. Miike, Phys. Rev. E **56**, 2367 (1997).
[21] L. M. Pismen, Phys. Rev. Lett. **78**, 382 (1997).
[22] K. Yoshikawa, T. Kusumi, M. Ukitsu, and S. Nakata, Chem. Phys. Lett. **211**, 211 (1993).
[23] O. Steinbock and S. C. Müller, J. Phys. Chem. A **102**, 6485 (1998).
[24] H. Miike, L. Zhang, T. Sakurai, and H. Yamada, Pattern Recogn. Lett. **20**, 451 (1999).
[25] L. Zhang, T. Sakurai, and H. Miike, Image Vis. Comput. **17**, 309 (1999).
[26] R. J. Field and M. Burger, *Oscillations and Traveling Waves in Chemical Systems* (Wiley, New York, 1985).
[27] R. J. Kaner and I. R. Epstein, J. Am. Chem. Soc. **100**, 4073 (1978).
[28] R. J. Field and R. M. Noyes, J. Chem. Phys. **60**, 1877 (1974).
[29] J. J. Tyson and P. C. Fife, J. Chem. Phys. **73**, 2224 (1980).
[30] J. P. Keener and J. J. Tyson, Physica D **21**, 307 (1986).
[31] L. D. Landau and E. M. Lifshitz, *Fluid Mechanics: Course of Theoretical Physics* (Pergamon, Oxford, 1959), Vol. 6.